

mole fraction of acetone. Molecular associations have been found to be positive in II and III.

Acetone has been mixed with nonpolar benzene, nearly nonpolar toluene, and associating ethylene glycol. Negative excess compressibilities are shown by the systems involving hydrogen bonding, these being large in those cases where one component is associated in the pure state (3). Acetone + ethylene glycol forms such a system and large negative values of excess compressibility have been recorded in this case which is indicative of strong interaction between the components of this mixture. The positive portion of the smooth curve of β_s^E shows a maximum at 0.9 mole fraction of acetone (Figure 1). Negative excess compressibilities have been observed for acetone + benzene (Figure 2) and acetone + toluene (Figure 3). Both benzene and toluene are nonpolar but their polarizability is high. The interaction in these cases seems to involve the π electrons on the aromatic rings.

Glossary

v	ultrasound velocity, $m\ s^{-1}$
β_s	isentropic compressibility, $cm^2\ dyn^{-1}$
ρ	density, $g\ mL^{-1}$
σ_x	standard deviation

n polynomial degree

Subscripts

E	excess function
calcd	calculated value
id	ideal value
exptl	experimental value
obsd	observed value

Literature Cited

- (1) Debye, P., Sears, F. W., *Proc. Natl. Acad. Sci. U.S.A.*, **18**, 410 (1932).
- (2) Deshpande, D. D., Bhatgadde, L. G., *J. Phys. Chem.*, **72**, 261 (1968); *J. Chem. Eng. Data*, **16**, 469 (1971).
- (3) Fort, R. J., Moore, W. R., *Trans. Faraday Soc.*, **61**, 2102 (1965).
- (4) Lagemann, R. T., Corry, J. E., *J. Chem. Phys.*, **10**, 759 (1942).
- (5) Prakash, S., Prasad, N., Prakash, O., *Indian J. Phys.*, **50**, 801 (1976).
- (6) Prasad, N., Prakash, S., *J. Chem. Eng. Data*, **22**, 49 (1977).
- (7) Prasad, N., Prakash, O., Singh, S., Prakash, S., *Ultrasonics*, **16**, 77 (1978).
- (8) Redlich, O., Kister, A. T., *Ind. Eng. Chem.*, **40**, 345 (1948).
- (9) Snyder, W. J., Snyder, J. R., *J. Chem. Eng. Data*, **19**, 270 (1974).
- (10) Tuomikoski, P., Nurmi, P., *Comments Phys. Math.*, **10**, 11 (1940).
- (11) Vilcu, R., Simion, A., *Rev. Roum. Chim.*, **21**, 177 (1976).
- (12) Weissberger, A., "Techniques of Organic Chemistry", Vol. 7, Interscience, New York, 1959, pp 315, 318, 362, 379.

Received for review October 26, 1978. Accepted July 30, 1979. Financial assistance from SCST (Lucknow) and UGC (Delhi) is gratefully acknowledged.

Thermal Conductivity of Gaseous Mixtures of Methane with Nitrogen and Carbon Dioxide

Peter L. Christensen and Aage Fredenslund*

Instituttet for Kemiteknik, Danmarks Tekniske Højskole, DK-2800 Lyngby, Denmark

Thermal conductivities of nearly equimolar, gaseous mixtures of methane with carbon dioxide and nitrogen are measured by using a coaxial cylinder conductivity cell. Results obtained in the same apparatus for pure methane are within 3% of the thermal conductivities predicted by using the correlation of Hanley et al.

Introduction

Knowledge of the thermal conductivities of natural gases and related mixtures is of central importance in the design of natural gas liquefaction plants and related processes. Several models have been proposed for the estimation of mixture thermal conductivities from pure-component conductivities only; see, for example, ref 1, Chapter 10. Due to the scarcity of experimental data, however, these models cannot be fully verified. In this work we report thermal conductivities of the gaseous mixtures methane-carbon dioxide and methane-nitrogen. These measurements supplement the results reported by Rosenbaum (2) for methane-carbon dioxide, which contain data at temperatures higher than those of this work. To our knowledge, thermal conductivities of the mixture methane-nitrogen have not been reported previously.

Thermal Conductivity Cell

The coaxial cylinder conductivity cell is constructed according to the principles given by Guildner (3). A schematic diagram of the cell is shown in Figure 1. The cell is constructed from

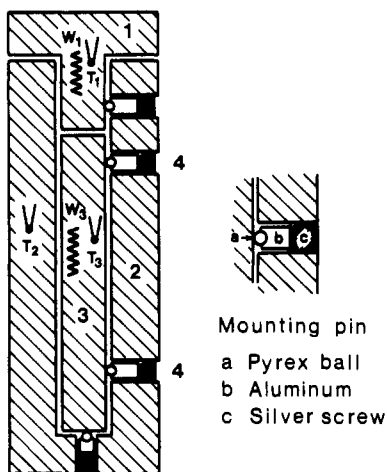
silver, and Pyrex sphere and aluminum holders are dimensioned such that their collective thermal expansion coefficient equals that of silver. The dimensions of the cell are as follows: emitter diameter = 14.98 ± 0.01 mm; emitter length = 83.59 ± 0.01 mm; conductivity gap = 0.52 ± 0.01 mm.

Experimental Section

The thermal conductivity cell is placed in the air thermostat described in ref 4. The cell is contained within a high-pressure steel cylinder. During operation, the space between the cell and the cylinder is occupied by the gas under investigation. The temperature of the air in the thermostat is maintained within 0.01 K of the desired temperature. When the resistances of the three thermistors have remained constant for at least 60 min, the values of the resistances are recorded and the voltage to the heaters in the emitter and heat guard is switched on. The electrical energy supplied to the two heaters is regulated such that the temperature rise in the emitter and heat guard becomes nearly equal. The difference between the emitter and heat guard temperature rise is calculated from

$$D_1 = T(R_3) - T(R_03) - [T(R_1) - T(R_01)] \quad (1)$$

$T(R)$ is an analytical expression giving the temperature as a function of the thermistor resistance; the function, based on standards supplied by the manufacturer, has the form of a polynomial. This approach is reasonable as long as the differences $[T(R_3) - T(R_03)]$ and $[T(R_1) - T(R_01)]$ are small. (R_01 = resistance of thermistor 1 before heating, R_03 = resistance of thermistor 3 before heating, R_1 = resistance of thermistor



1. Heat guard
2. Receiver
3. Emitter
4. Mounting pins
 W_1, W_3 Heaters
 T_1, T_2, T_3 Thermistors

Figure 1. Thermal conductivity cell measurement.

1 during heating, R_3 = resistance of thermistor 3 during heating.)
The difference between the temperature rise of the emitter and receiver, D_2 , is found similarly:

$$D_2 = T(R_3) - T(R_03) - [T(R_2) - T(R_02)] \quad (2)$$

The thermal conductivity of the gas can now at any given time t and in the absence of corrections be calculated by

$$\lambda(t) = \frac{Q}{K_1 \cdot D_1(t) + K_2 \cdot D_2(t)} \quad (3)$$

where λ = thermal conductivity (mW/mK), Q = emitter effect (mW), K_1 = constant corresponding to the gas layer between the heat guard and emitter (area divided by distance) (m), and K_2 = constant corresponding to the gas layer between receiver and emitter (area divided by distance) (m).

Corrections

Temperature Drift. If the emitter temperature varies with time, there is a difference between the added electrical effect and the emitted effect:

$$Q_{\text{emitted}} = Q_{\text{added}} - (\text{Cap})(dT/dt) \quad (4)$$

where Cap is the thermal capacity of the emitter and dT/dt is the temperature drift.

Convection. If one assumes steady state, laminar convection in the cell annulus, the following expression for the heat transfer due to convection holds:

$$Q_{\text{convection}} = A \cdot f(\alpha, \rho, C_p, \eta) \cdot \Delta T^2 \quad (5)$$

where A = a constant characteristic of the cell (m^2/m), α = thermal expansion coefficient (K^{-1}), ρ = density (kg/m^3), C_p = heat capacity (J/kg), η = viscosity ($\text{kg}/(\text{m s})$), ΔT = temperature difference between emitter and receiver (K), and f is a function which is assumed to attain a constant value within a small temperature range. Hence $Q_{\text{convective}}/\Delta T$ will increase pro-

Table I. Thermal Conductivity for Gaseous Methane and Ethane

	T_0 , K	P , atm	ρ , mol/L	λ_0 , mW/(m K)		
				this work	ref 5	% dev
CH ₄	249.21	100.95	7.283	48.47	47.04	-2.97
	248.94	65.85	4.148	39.54	38.75	-2.0
	258.82	52.82	2.937	37.25	37.11	-0.38
	260.24	53.15	2.931	36.67	37.27	1.64
	228.99	16.62	0.954	28.25	28.93	2.41
C ₂ H ₆	248.54	6.32	0.316	29.65	29.54	-0.37
	226.92	5.41	0.324	15.09		
	245.60	5.92	0.322	17.11		
	257.84	6.26	0.321	18.35		

Table II. Thermal Conductivities for Methane-Carbon Dioxide ($x_{\text{CH}_4} = 0.5061$)

T_0 , K	P , atm	ρ , mol/L	λ_0 , mW/(m K)
228.13	14.69	0.885	20.54
238.14	15.52	0.886	21.47
246.84	16.18	0.883	22.23
254.39	16.93	0.891	22.61
267.12	17.68	0.876	24.45
238.23	10.54	0.579	20.60
246.77	10.97	0.578	21.77
266.93	11.98	0.577	23.39
228.32	2.61	0.142	19.14
238.51	2.74	0.142	19.80
246.75	2.82	0.142	20.65
253.94	2.91	0.142	21.68
266.92	3.06	0.142	23.02
272.07	3.12	0.142	23.28

portionally with ΔT , and the following expression holds:

$$\lambda = \lambda_0 + \frac{A \cdot f(\alpha, \rho, C_p, \eta) \cdot \Delta T}{K_2} \quad (6)$$

where λ_0 is the thermal conductivity in the absence of convection.

Heat Emission from the Cell. When the cell heaters are switched on, a certain amount of energy is transferred from the outer walls of the cell to the gas between the cell and the steel cylinder. Hence the cell will be heated slightly. If the conduction between the emitter and the receiver and the receiver and the gas in the steel cylinder both increase proportionally with the respective temperature differences, the cell temperature T , defined as the average between the emitter and receiver temperatures, will increase proportionally with ΔT :

$$T = T_0 + B \Delta T \quad (7)$$

where B is a constant and T_0 is the temperature corresponding to the conductivity λ_0 .

For each reported value of the thermal conductivity we have carried out measurements for several values of ΔT . If there is no transition between laminar and turbulent convection—a safe assumption in this case—the thermal conductivity and the corresponding temperature may be determined by using linear regression as indicated by eq 6 and 7. The reported thermal conductivities and temperatures are those corresponding to $\Delta T = 0$, in which case $\lambda = \lambda_0$ and $T = T_0$.

Results

In order to check the accuracy of the results, we carried out measurements for pure methane, for which an accurate correlation based on a large number of experimental data points exists (5). Hanley et al. report an average deviation between their correlation and the experimental values of 5%. Our experimental results for methane are shown in Table I, which

Table III. Thermal Conductivities for Methane-Nitrogen ($x_{\text{CH}_4} = 0.5102$)

T_0 , K	P , atm	ρ , mol/L	λ_0 , mW/(m K)
221.32	61.47	4.085	30.39
227.95	64.73	4.114	31.02
237.78	71.93	4.314	32.70
246.34	76.13	4.331	33.41
253.19	79.84	4.367	34.22
266.58	85.92	4.361	34.47
271.76	86.24	4.254	36.39
246.14	23.58	1.223	27.18
238.19	4.32	0.223	25.04
229.97	2.90	0.155	24.63
248.42	3.07	0.151	26.66

in addition contains a few results for ethane. The deviation between the results of this work and the correlation by Hanley et al. is in no case larger than 3%.

Tables II and III show the measured thermal conductivities for the gaseous mixtures methane-carbon dioxide ($x_{\text{CH}_4} = 0.5061$) and methane-nitrogen ($x_{\text{CH}_4} = 0.5102$).

In Tables I, II, and III, the densities are calculated by using the highly accurate corresponding states correlation by Mollerup (6).

Acknowledgment

The authors are thankful to B. Johnsen for assistance with the experimental work and to J. Mollerup for carrying out the density calculations.

Literature Cited

- (1) Reid, R. C., Prausnitz, J. M., Sherwood, T. K., "The Properties of Gases and Liquids", McGraw-Hill, New York, 1977.
- (2) Rosenbaum, B. M., Thodos, G., *J. Chem. Phys.*, **51**, 1361 (1969).
- (3) Guildner, L. A., *J. Res. Natl. Bur. Stand., Sect. A*, **No. 66A**, 333 (1962).
- (4) Grausó, L., Fredenslund Aa., *Ber. Bunsenges. Phys. Chem.*, **61**, 1089 (1977).
- (5) Hanley, H. J. M., McCarty, R. D., Haynes, W. M., *Cryogenics*, **15**, 413 (1975).
- (6) Mollerup, J. M., *Adv. Cryog. Eng.*, **20**, 172 (1975).

Received for review October 30, 1978. Accepted May 22, 1979.

Solubility of α -HgI₂ in Dimethyl Sulfoxide-Methanol and Dimethyl Sulfoxide-Ethyl Acetate Mixtures

J. Joly, I. Nicolau,* and M. Armand

Laboratoire D'Electronique et de Technologie de l'Informatique, Division Cristallogénèse et Recherche sur les Matériaux, Commissariat à l'Énergie Atomique, Centre d'Etudes Nucleaires de Grenoble, 85 X, 38041—Grenoble Cedex, France

The solubility of α -HgI₂ in dimethyl sulfoxide-methanol mixtures was determined in the range of 0.6–0.8 dimethyl sulfoxide mole fractions from 25 to 40 °C (for 35 °C it was determined in the full range of mole fractions). The solubility of α -HgI₂ in ethyl acetate and in dimethyl sulfoxide-ethyl acetate mixtures was determined up to 0.1287 dimethyl sulfoxide mole fraction in the range 40–60 °C.

Introduction

We have recently developed a new method of growing single crystals of α -HgI₂ in solution using HgI₂-Me₂SO (dimethyl sulfoxide) molecular complexes (5).

To better understand and control the crystallization process of α -HgI₂ by means of its molecular complexes, we have previously studied the donor-acceptor type interaction between HgI₂ and various basic solvents (2) and we now study the solubility of α -HgI₂ in Me₂SO-MeOH (methanol) and Me₂SO-EA (ethyl acetate) mixtures. As we have found formerly, Me₂SO acts as a complexing agent against HgI₂. The ranges of temperatures and concentrations investigated have been restricted to those useful for growing single crystals of α -HgI₂.

Experimental Section

Materials. Analytical grade α -HgI₂ from Merck was further purified by three successive recrystallizations in solution of Me₂SO-MeOH (5). Analytical grade dried Me₂SO from Merck and analytical grade EA from Carlo Erba have been used without further purification. Analytical grade MeOH from Prolabo was further rectified on a packed column to eliminate its water content.

Procedure. For measuring the HgI₂ concentration of saturated solutions, a straight-forward gravimetric analysis was

chosen. Different Me₂SO-solvent mixtures, in volumes of about 100 mL, were prepared by weighing in bottles of 200 mL, tightly stopped by screwing on plastic stoppers supplied with Teflon gaskets. α -HgI₂ in excess was then introduced and the bottles were kept in a thermostated bath for 2 weeks to reach saturation, stirring the mixture twice a day. The temperature was controlled within ± 0.01 °C. Samples of 5 mL of saturated solution have been pipetted out from the bottles and kept in closed weighing bottles. The samples were evaporated to dryness in a drying chamber under vacuum for a few hours at room temperature to evaporate the most volatile solvent (MeOH or EA) and then 12 h at 50 °C to evaporate Me₂SO. The samples were accurately weighed before and after solvent evaporation. New samples of saturated solution were again pipetted out from the bottles after 2 weeks and worked out as above. The data listed in tables are averages among many close values obtained from many samples. The experimental values do not differ from these data more than 1% for the Me₂SO-EA mixtures and more than 0.5% for the Me₂SO-MeOH mixtures.

Results

The solubility of α -HgI₂ in Me₂SO-MeOH mixtures was investigated in the range of 0.6–0.8 Me₂SO mole fractions, $X_{\text{Me}_2\text{SO}} = n_{\text{Me}_2\text{SO}}/(n_{\text{Me}_2\text{SO}} + n_{\text{MeOH}})$, from 25 to 40 °C and in the full range of Me₂SO mole fractions at 35 °C.

The following empirical parabolic relation fits the experimental data within the experimental accuracy ($\pm 0.25\%$):

$$R_{\text{HgI}_2} = -(3.03 \times 10^{-2}) + (5.4 \times 10^{-4})(t - 25) + [(1.735 \times 10^{-1}) + (2 \times 10^{-4})(t - 25)]X_{\text{Me}_2\text{SO}} + (3.95 \times 10^{-1})X_{\text{Me}_2\text{SO}}^2 \quad (1)$$

The temperature t is in °C and the α -HgI₂ mole ratio R_{HgI_2} is $n_{\text{HgI}_2}/(n_{\text{Me}_2\text{SO}} + n_{\text{MeOH}})$. Experimental and calculated data are given in Table I. Figure 1 shows the complete isotherm of